Journal of
Sedimentary
Research

Journal of Sedimentary Research, 2022, v. 92, 739–750
Research Article
DOI: 10.2110/jsr.2022.028

MICROBIAL-MAT COLONIZATION OF MODERN GRAVEL DEPOSITS IN A SILICICLASTIC COASTAL SETTING

JERÓNIMO PAN,[1,2,3] DIANA G. CUADRADO,[1,4,5] AND NORA K. NOFFKE[6]
[1]CONICET, Consejo Nacional de Investigaciones Científicas y Técnicas, Argentina
[2]IGCyC, Instituto de Geología de Costas y del Cuaternario, Mar del Plata 7600, Argentina
[3]IIMyC, Instituto de Investigaciones Marinas y Costeras, Mar del Plata 7600, Argentina
[4]IADO, Instituto Argentino de Oceanografía, Bahía Blanca 8000, Argentina
[5]Departamento de Geología, Universidad Nacional del Sur, Bahía Blanca 8000, Argentina
[6]Department of Ocean and Earth Sciences, Old Dominion University, Norfolk, Virginia 23529, U.S.A.
e-mail: jeronimopan@gmail.com

ABSTRACT: **Microbial mats are layered consortia of microorganisms colonizing surface sediments that alter their physical and chemical characteristics. The northern Patagonia coastline (Argentina) includes gravel deposits (termed *rodados Patagónicos*) accumulated during the Pleistocene and Holocene by high-energy hydrodynamic processes. In this area, surface sediments in a relict tidal channel (Paso Seco; 40° 38′ 27″ S, 62° 12′ 55″ W) are extensively colonized by microbial mats, appearing to overgrow exposed gravel deposits. To date, such substrates have not been reported as suitable for the development of microbial mats. The objectives of this paper are: 1) to describe the mechanisms of microbial baffling, trapping, and binding of sedimentary particles, and biostabilization that enable epibenthic microbial mats to develop on gravel substrates, 2) to relate microbial mat growth to a variety of hydrodynamic conditions, and 3) to describe resulting microbially induced sedimentary structures (MISS). Our hypothesis is that the alternation of episodic seawater flooding, stagnation, and draining with subsequent subaerial exposure and desiccation are the controlling factors for mat development on gravel. Once stagnant, mud-size sediment particles settle from suspension. At the same time, an initial biofilm may become established on the bottom, using the fine-grained material as substrate. Subsequently introduced particles are baffled, trapped, and bound into the developing biofilm matrix. During the Austral winter comparatively higher values for chlorophyll *a* and organic matter point towards increased growth of the microbial mat during this season. With increasing coherence, the developing microbial mat may encroach onto individual pebbles, ultimately engulfing them. Eventually, a mature, epibenthic microbial mat levels the sedimentary surface. Hydrodynamic reworking during flooding produces MISS such as mat chips and flipped-over mats.**

INTRODUCTION

Biofilms may grow on sedimentary surfaces into layered microbial mats that include cells and their secreted exopolymers as well as mineral particles; the latter are derived from the substrate and are dragged upward during growth and thickening of the biofilms (Noffke et al. 1997; Fenchel and Kühl 2000; de los Ríos et al. 2004; Kaźmierczak et al. 2015). The microbial mats developing in tidal flats are commonly dominated by cyanobacteria. From a bioenergetic point of view, the oxygenic photosynthesis carried out by these phototrophs constitutes the "motor" driving most metabolic pathways represented in such a mat (Stal et al. 1985; Pan 2021). Aside from cyanobacteria, other Bacteria, Archaea (Bolhuis and Stal 2011), and single-celled Eukarya (Edgcomb et al. 2014) occur. In siliciclastic settings, where physical sedimentary processes, rather than chemical precipitation of minerals, are preeminent, microbial mats form microbially induced sedimentary structures (MISS) (Noffke et al. 2001; Noffke 2010). Whereas microbial mats in tidal flats have been reported to commonly colonize sandy substrates, this contribution presents microbial mats covering gravel substrates.

In Argentina, extensive tidal flats include areas composed of gravel deposits known as *rodados Patagónicos* (Martínez and Kutschker 2011). They are attributed to past high-energy hydrodynamic processes that took place at the end of the last glacial event, when large amounts of water were released from the melting of the Cordilleran ice sheet. At Paso Seco, northeastern Patagonia, these gravel deposits are widely overgrown by microbial mats. At first, such colonization on gravel may seem striking, since previous evidence indicates that microbial mats commonly form in fine, sandy sediments, rich in quartz (Noffke 2000, 2010). In addition, a laboratory experiment proved that cyanobacteria prefer sandy sediments (Watermann et al. 1999), and it has been experimentally demonstrated that microbial mats in culture are much more effective at trapping fine grains than larger grains (Frantz et al. 2015).

The objective of this paper is to describe how microbial communities develop on sediments of pebble size, and which role biomass accumulation and baffling, trapping, and binding behaviors play. Our hypothesis is that an overlap of hydrodynamic, sedimentary, and microbial processes control mat development on pebble deposits, involving: 1) frequent flooding by seawater depositing sand-size material onto the gravels, 2) fallout of mud-

1527-1404/22/092-739

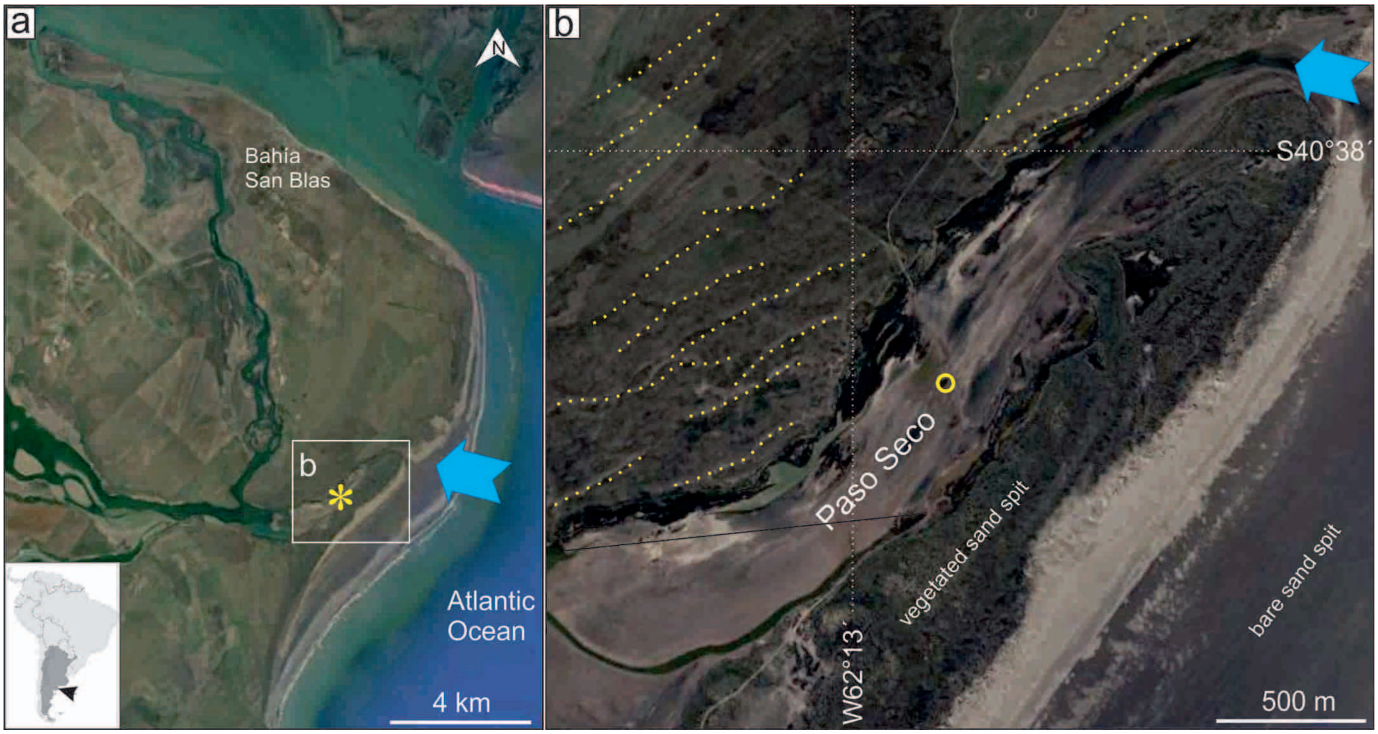

Fig. 1.—Satellite image of the study site. **A)** The Paso Seco area is in the inset box, marked by a star. The blue arrow points to the inlet of the relict tidal channel through which seawater enters the site during storm surges, and the predominant flow direction. **B)** Close-up view of Part A. Gravel ridges are highlighted in dashed yellow lines. The yellow circle indicates the pond where the study was carried out; blue arrow, same as in Part A.

size sediment particles suspended in the stagnant water following inundation, and 3) anchoring of a biofilm fabric in sand and baffling and trapping of fine sediment by a rapidly growing microbial mat. Thus, this contribution will illuminate how microbial mats colonize seemingly inhospitable substrates such as pebbles.

MATERIAL AND METHODS

Study Site

Paso Seco (40° 38′ 27″ S, 62° 12′ 55″ W; Fig. 1) is in the surrounding area of Bahía San Blas (Argentina) that is characterized by gravel and sand deposits. The region has an average annual rainfall of less than 300 mm, and the potential evapotranspiration commonly exceeds precipitation (Ferrelli et al. 2012). Paso Seco is a relict tidal channel of Pleistocene age (Trebino 1987) with its northern margin formed by vegetated pebble ridges of Holocene age, while the southern margin is formed by a younger vegetated sand spit. The longshore sand transport forming the sand spit narrowed the connection of the tidal channel with the coastal ocean (Espinosa and Isla 2011) where progradation processes prevailed (Fig. 1B). While the tidal channel is no longer active, the seawater overfloods the sand spit during severe storms. The frequency of seawater flooding is related to a combination of oceanographic and atmospheric factors (e.g., atmospheric disturbance located on the Atlantic Ocean, wave period and height in deep water, spring tides) that, when occurring jointly, produce a storm surge pushing seawater past the sand spit where microbially colonized sediments are common (Stempels Bautista et al. 2019). Due to a topographic low, seawater inundates the microbial mats followed by evaporation giving the area some characteristics of a saline basin (Perillo et al. 2019). The analysis of loose grains from sand sediments forming the relict tidal channel reveals the presence of quartz, feldspars, pyroxenes (hypersthene and augite), and opaque grains. X-ray diffraction analysis corroborates the presence of evaporite minerals, such as halite and gypsum, as well as light minerals such as quartz, feldspars, and muscovite (Maisano et al. 2016).

The gravel deposits known as *rodados Patagónicos* are accumulations of well-rounded pebbles in a sandy, silty, or clayish matrix, rarely with carbonate cement (Martinez et al. 2009). Their presence along the coastline of Bahía San Blas is related to past shoreline transport, following the elevation of Southern Hemisphere shorelines by glacio-isostatic adjustment surrounding Antarctica (Rutter et al. 1989). At present, the *rodados Patagónicos* at our study site are part of a depositional mosaic consisting of upper Quaternary beach gravel deposits (originally described by Witte 1916) and Holocene sand dunes (Trebino 1987); they are not being reworked by the modern hydrodynamic regime. The pebbles are predominantly basic and mesosilicic volcanic and acid plutonic rock. They may reach up to 5 cm in maximum diameter. Their roundness points to a fluvio-glacial origin during the late Cenozoic, when surface drainage networks of relatively high energy existed in the region (Martínez and Kutschker 2011).

Centimeter-thick, cohesive epibenthic microbial mats colonize an area of 1.14 km^2 (3.3 km × 0.4 km) on the bottom of the relict tidal channel. However, where flood currents cross the area, hydraulic reworking causes mat material to be displaced and MISS such as flipped-over mats, mat chips, roll-ups, and erosional pockets form (Cuadrado et al. 2015; Maisano et al. 2019). Microbiologically, the mats of Paso Seco are dominated by filamentous cyanobacteria (the vast majority pertain to the order Oscillatoriales, with some representatives of the order Nostocales; Cuadrado and Pan 2018). Mats in this environment withstand desiccation over periods > 10 days, with average maximum summer high temperatures of 27°C (reaching up to 40°C), and hypersalinity in semipermanent ponds (average $S = 71.8$ on Austral summer, and $S = 44.5$ in Austral winter).

Microbiological Sampling and Sample Processing

Samples of intact epibenthic microbial mats removed from gravel were taken on two fieldtrips (15/12/2020 and 15/7/2021, corresponding to Austral summer and winter, respectively), and transported to the laboratory in air-tight containers. The samples were approximately 7 cm × 7 cm × 1.6 cm in size. Upon arrival in the laboratory, vertical sections through microbial mats were cut to study their layered depth profile, under a stereomicroscope (Leica Microsystems, model Stereozoom S9D, equipped with a KL300 LED source). The uppermost 2 mm (corresponding to the oxic layers) and the underlying –2 to –4 mm of the mat (anoxic layers) of the microbial mat, as well as the topmost 2–3 mm of the biofilm forming a rim where the mat margin "encroaches" underlying gravels, were sampled with micro-corers (inner diameter 6 mm). Additionally, the thin biofilm covering individual pebble surfaces was scraped with a sterilized scalpel and preserved for qualitative microbiological analysis. All microbiological samples were preserved in 5% acidic Lugol's iodine solution (stock solution prepared with natural filtered seawater) in 50-ml vials and subject to shaking and 5 min of mild-intensity ultrasound (Testlab ®, model TB010) by immersing the samples in a cold-water bath, to disaggregate the mat fabric. Aliquots of the resulting slurry were transferred onto covered glass slides for observation under a light microscope (Zeiss, model Primo Star HAL/LED source; or Nikon, model YS2-T) at 200–400× magnification, after Pan et al. (2017). Cyanobacteria were identified morphologically; therefore, reference is made to morphogenera or morphospecies (Komárek and Hauer 2013). A semiquantitative estimate of cyanobacterial abundance was based on the proportion of the microscope field covered by the filaments (after Stal et al. 1985). Diatoms (single-celled eukaryotes) were identified to the lowest taxonomic level possible by light microscopy, and their ecological features regarding habitat preference, life form, and salinity tolerance were typified after Denys (1991) and Vos and de Wolf (1993). No other microbial taxonomic groups were identified for the purposes of this study.

Sediment Analysis

Organic matter was determined with the weight-loss-on-ignition method, for which mat samples were dried for 48 h and then combusted at 550°C for 6 h in a muffle furnace (Blakemore et al. 1987). Photosynthetic pigments in sediment (chlorophyll *a*, a proxy for autotrophic biomass expressed as μg Chl a g^{-1} sediment) was estimated from $n = 3$ cylindrical sediment cores (polypropylene; inner diameter = 6 mm, height = 10 mm) that were sliced with a sterilized scalpel into two depth-profile layers (namely 0 to –2 mm, and –2 to –10 mm). Pigment extraction was done in a solvent mixture of methanol and acetone 50:50% vol/vol, for 24 h at –20°C, and measured spectrophotometrically under dim-light conditions (BioTek Instruments, Epoch 2 microplate spectrophotometer). Chlorophyll *a* content was calculated after Lorenzen (1967).

The particle size of the microbial mat growing over gravels was measured on two fractions, namely 0 to –2 mm, and –2 to –4 mm, by laser diffraction using a particle analyzer (Malvern Panalytical, model Mastersizer 2000^{TM}). The resolution range for particles was between 0.2 and 2,000 μm (i.e., colloids to sand), previously oxidizing the organic matter of the sample with a 65% H_2O_2 solution and heating.

Hydrodynamics

The frequency and magnitude (i.e., water-column height) of inundation and the residence time of each flooding of the sedimentary flat was recorded by a water-level logger (HOBO, model U20; 2.5 cm diameter and 15 cm length; Onset Computer Corporation, Bourne, MA, USA). The logger was deployed into the lumen of a 40-cm-long perforated PVC pipe, buried vertically in the microbial-mat planar surface. It recorded the pressure (water column + atmospheric) and water temperature every 10 min. These data were corrected subtracting atmospheric pressure, which was measured with another HOBO placed on an upper topographic level, to obtain only data on water-column height over the sedimentary surface and variation of groundwater level. The water-level records show the groundwater variation below the mat surface, the frequency of inundations from the sea that enter the study zone, and how much the water column rises over the mat surface.

RESULTS

Epibenthic Microbial Mats Colonizing Gravel Deposits

Epibenthic microbial mats develop on gravel substrates in topographically positive areas of the sediment surface, sometimes adjacent to depressions that are semipermanently filled by seawater (Fig. 2A, B). When covered by a shallow water column (< 10 cm) or even just a sheet of water, cyanobacterial metabolism caused gas bubbles as visible in the example of a blue-green mat surface in Figure 2C. The degree of lateral mat expansion seems to correlate with the micro-topography generated by the height of individual pebbles relative to the sediment surface. In some cases, pebbles may be barely covered by a mat that in this case forms a rim (1 in Fig. 2C), or microbial mat may either cover individual pebbles partially (2 in Fig. 2C), or the pebbles may completely covered by the mat, which then become invisible (3 in Fig. 2C). The photos depict the steps from onset of gravel colonization to the final cover of pebbles. First, the mat encroaches the pebble from all sides and a mat rim is formed around the pebble; later the mat growth proceeds to engulf the pebble centripetally. Episodic strong flood currents may cause ripping and overfolding of the microbial mat (Fig. 2D). Large-scale fold-overs are conspicuous features in field-view (see Fig. 2A, B). Either the fold-overs may retain pebbles that had been incorporated into the mat fabric, or the detached mats show negative moulds of pebbles from the substrate (Fig. 2D).

Hydrodynamic Regime and Biofilm Evolution

The hydrodynamic regime at Paso Seco is characterized by episodic seawater flooding only during storms (the rhythm of inundation is non-periodic) resulting in variable residence time of the seawater, as well as seasonal variation of the groundwater level. As an example, an annual water level-record is shown in Figure 3A, where the flat was flooded at least once each month, often remaining stagnant for several consecutive days. In Austral winter, once the seawater recedes, the groundwater level remains close to the surface for several days or months (see red frame in Fig. 3A). In contrast, the groundwater rises and falls several centimeters below the sediment surface the rest of the year. Thus, groundwater level drops up to 30–40 cm in Austral spring and summer, when the microbial-mat surface is exposed for several days. Solar radiation and subaerial exposure promote evaporation, which leads to mat desiccation (see Fig. 2A). In contrast, floods (creating a water column ≥ 40 cm over the channel flat) may mechanically disrupt epibenthic mats, and displace large parts, even generating entangled pieces of mats (Fig. 3B). Also, the microbial mat, if remaining under stagnant water, may be recolonized by a pioneering biofilm, causing a golden-tinged surface coloration and gas bubbles (Fig. 3B). Depending on the extent of exposed surfaces, such pioneering biofilms may occur over large areas (Fig. 3C). However, where microbial mats cover the sediment surface, water stagnation causes reticulate patterns of ridges and tufts on the mat surfaces (Fig. 3D).

The physiognomy of the microbial mat surface adjacent to gravels is also affected by seasonal differences. During Austral summer months, when surface sediments are more frequently subject to desiccation, the rim forming around individual pebbles remained distinctly bound to pebble grains (Fig. 4A, B). Also indicative of the prevailing dry condition in Austral summer, there are halite crystals visible covering both the pebble and the mat surface. Conversely, in Austral winter, when a stagnant film of

Fig. 2.—Field view of the study area and associated MISS. **A)** Negative and positive topography colonized by microbial mats, during Austral summer. Fold-overs of epibenthic microbial mat expose areas abundant in gravel deposits. **B)** Idem in Austral winter. **C)** Different stages of microbial mat development: widely exposed gravel (1), with partially exposed gravel (2), and completely covering gravel deposits (3). The ongoing engulfing of individual pebbles is indicated by yellow arrows. The sporadic inundation by water is evidenced by the presence of the halophyte *Sarcocornia perennis* (upper and lower right corners). **D)** Detail of a fold-over structure, in which the negative casts of once covered pebbles (1) might be seen on the underside (2).

water covers the microbial mats for periods of ~ 14 days and longer, biofilm "engulfing" individual pebbles become a common feature. This highly hydrated biofilm presenting a characteristic rim or border (Fig. 4C) was sampled, but once dried in the laboratory, the surface dehydrated and shrank, thus revealing a greater surface of the pebble (Fig. 4D).

The pioneering biofilm that forms under stagnant seawater in sandy sediment (Fig. 5A, B) has the same appearance when covering individual pebbles (Fig. 5C, D), and often shows a reticular pattern as well. The stagnant water column of a few centimeters depth (or even a thin lamina of overlying seawater) provides an adequate environment for microbial growth, starting first with this hydrated biofilm rims engulfing and growing over pebbles (Fig. 5C, D). Of interest is the sequential colonization of pebbles analyzed in a micro-topographic transect (24 cm long), directed from water-covered topographic lows to highs. Under stagnant water, individual pebbles are covered by mud and biofilm (Fig. 5C, D). Moreover, there are differences in adjacent individual pebbles in the degree of biofilm colonization, with respect to the relative position of the pebbles in a hypothetical planar surface. Hence, a pebble resting on the surface may be covered by mud and a fine biofilm (1 in Fig. 5D); meanwhile, a pebble placed in a lower topographic level shows the incipient formation of a rim (2 in Fig. 5D). The pebbles located buried in a deeper position have a thick biofilm nearly covering them (3 and 4 in Fig. 5D). In that case, the rim around the pebbles may "flap" by the oscillating movement of water (refer to video 1 in Supplemental Material). Some centimeters apart, at a higher topographic level, moist pebbles (no longer covered by water) are engulfed by a wet biofilm, producing copious gas

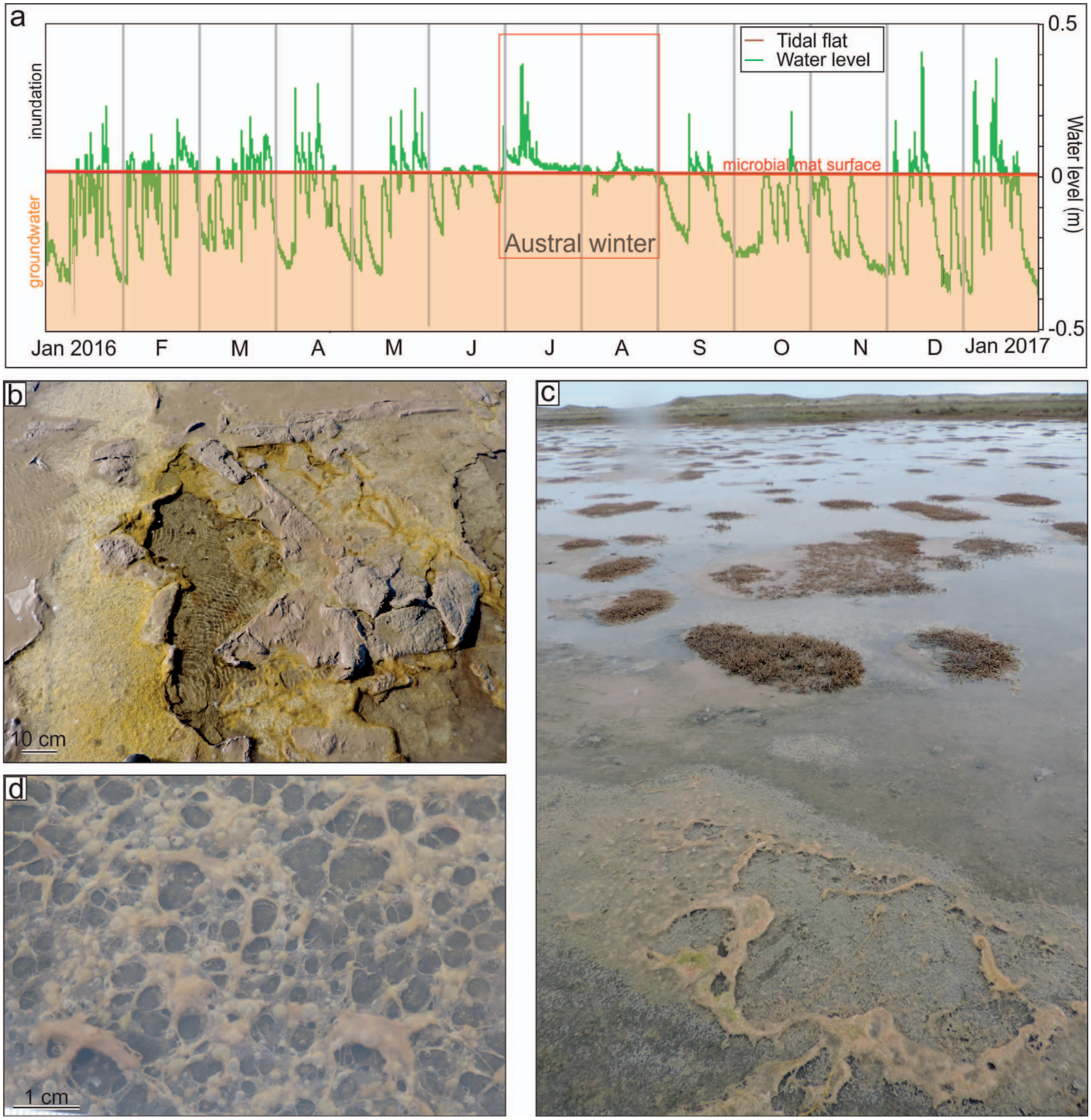

Fig. 3.—Inundation record and general aspect of relict tidal channel after flooding. **A)** Water-level record over a year. Inset box comprises Austral-winter months when the water table remains closer to the sediment surface. Inundations from seawater intrusion are shown as peaks above the sediment surface; groundwater variation is shown below the sediment surface (colored area). **B)** Deformation structures that arise from hydrodynamic processes during flooding. Golden color indicates biofilm colonization over a disturbed, convoluted microbial mat. **C)** Large areas of diatom biofilm recolonization at the foreground (developed in the presence of a thin layer of water); background with patches of *Sarcocornia perennis*, a halophyte whose distribution indicates sporadic inundation by seawater. **D)** Close-up of microbial biofilm reticulates formed from biomass growth during latency periods of seawater stagnation.

bubbles during the daytime (Fig. 5E). After being subject to increasing solar radiation (from Austral mid-winter to spring), a well-developed microbial mat is visible, as the last stage of the evolution of the pioneer biofilm, covering each pebble in part or completely (Fig. 5F).

Microbiological Characteristics of Biofilms and Microbial Mats

In microbial mats, the size of the mineral particles interwoven in the microbial matrix shows a bimodal distribution with fine sediment (silt and

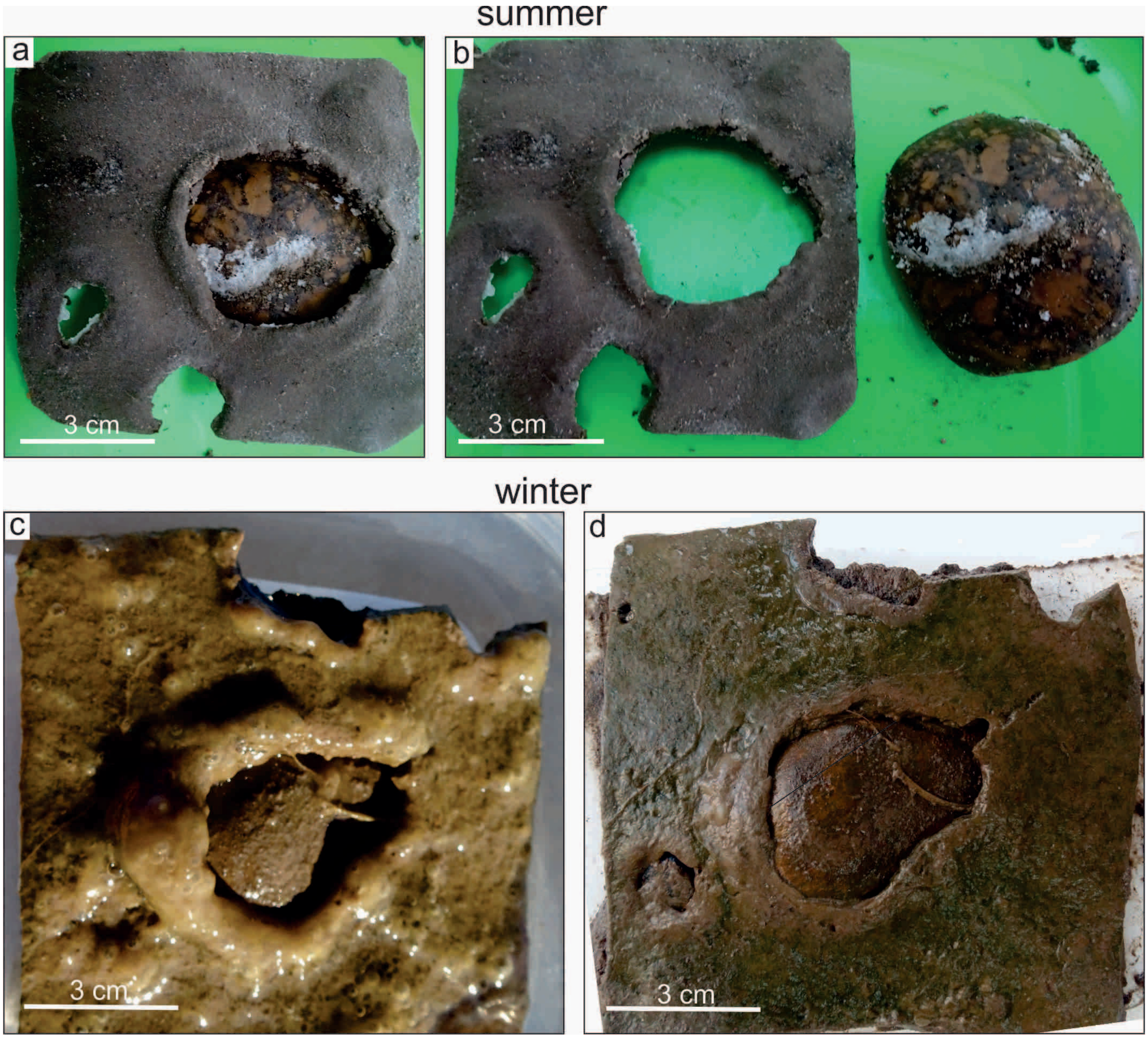

Fig. 4.—Actual field samples on which sedimentological and microbiological analyses are based. **A)** Austral-summer samples on arrival in the laboratory. **B)** Same as Part A after removing the pebble engulfed by the mat. Note halite crystals on the mat and pebble surface. **C)** Austral-winter sample showing a hydrated rim around an individual pebble (photograph taken in the field). **D)** Same as in Part C on arrival to the laboratory. The rim had decreased in size, exposing a greater surface of the pebble.

clay) fractions dominating both in the upper (0 to –2 mm) and underlying (–2 to –4 mm) layers of the microbial mat, and a fine sand fraction (200 µm diameter) being conspicuous in the upper layers (Fig. 6A). When examined under a stereomicroscope, the epibenthic mat presented typical layering (Fig. 6B). The uppermost 2 mm (conspicuously distinguished as the oxic layers) forms a very cohesive mat fabric of very densely intertwining filaments of the cyanobacterium *Coleofasciculus chthonoplastes* (Fig. 6C, D), which is also the dominant species by biomass. When observed under a light microscope, clumps of organic matter fill the few spaces unoccupied by trichomes, almost all of which are composed of living filaments in the uppermost 2 mm, though a few empty sheaths occurr. In Austral-winter samples, few trichomes and hormogonia of *Oscillatoria* sp. and accompanying filaments of the slender cyanobacterium *Leptolyngbya* sp. were also present. In Austral-summer samples, only a few pennate diatoms (*Navicula phyllepta* and *Navicula gregaria*) were found in the topmost 2 mm of the mat at very low densities, while in Austral-winter samples, the dominant pennate diatom was *Nitzschia sigma*. In samples from anoxic strata (–2 to –4 mm) *C. chthonoplastes* remained the dominant cyanobacterium, but empty sheaths of *C. chthonoplastes* appeared in a larger proportion compared to complete trichomes (i.e., with chlorophyll-containing filaments and enveloping sheaths; Fig. 6E, F). In Austral-summer samples, empty sheaths corresponding morphologically in their dimensions to the morphogenus *Symploca* were also found in this layer, but no pennate diatoms were recorded; conversely, in Austral-winter samples, *Leptolyngbya* filaments were also present and pennate diatoms were represented by several species (see Table 1), of which *N. sigma* was

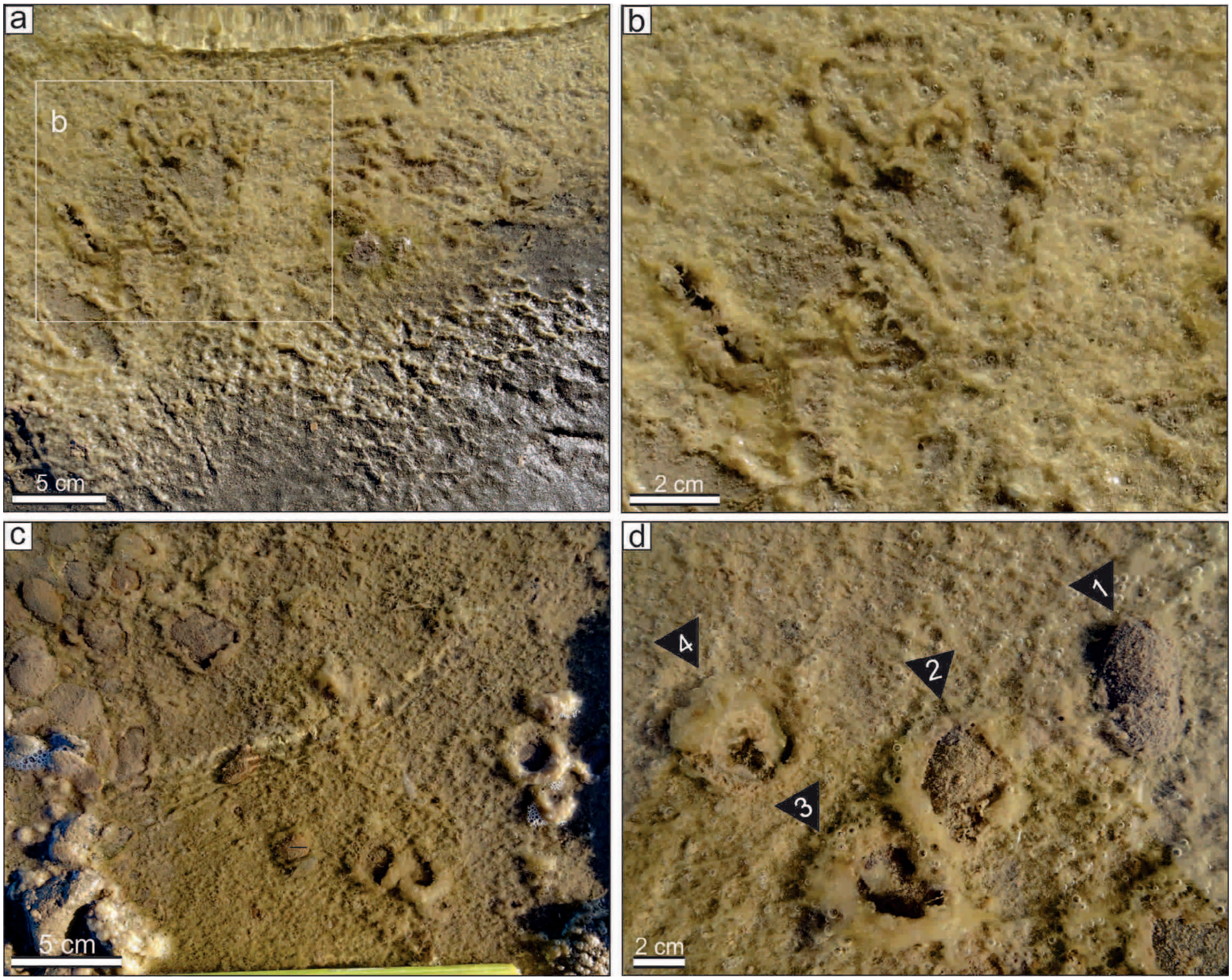

Fig. 5.—Biofilm colonization in sand and gravel substrate**.** **A)** Colonization of sand covered by a film of water (wind wave at the top). **B)** Close-up of Part A. **C)** Immersed biofilm colonization on a gravel substrate. **D)** Difference in colonization as a function of the position of pebbles in a submerged pond. (1) points an individual pebble on the surface with fine sediment coverage without rim. (2) points an individual pebble in a deeper position with an incipient formation of a rim. Thicker rim in (3) and nearly covered by biofilm in (4). **E)** Exposed colonization in moisty biofilm between pebbles; inset shows gas bubbles at a higher magnification. **F)** Dry microbial mat covering a gravel substrate.

the most abundant. In general, the majority of diatoms found in microbiological samples were raphid species that have affinities for marine and marine–brackish salinities, and epiphytic, epipelic, tychoplanktonic life forms, with two species being aerophilous. Regarding habitat preferences, most species found are characteristic of periodic water or moist–wet subaerial habitats (Table 1).

In microbiological samples of the mat rim encroaching individual pebbles, *C. chthonoplastes* was also the dominant cyanobacterium. Some filaments of *Symploca* sp. (2.5 µm in diameter, enveloped in thin sheaths) were found at much lower densities in Austral-summer samples, while trichomes and hormogonia of *Oscillatoria* sp. and filaments of *Leptolyngbya* were present in Austral-winter samples. Fewer diatom species were found near the rim in Austral-summer samples, while the diversity of pennate diatoms was much larger in Austral winter (Table 1). The microbiological analysis of the material scraped from the surfaces of individual pebbles was dominated by the pennate diatoms *N. sigma* and *N. palea*, including few cyanobacteria (*Leptolyngbya* and *Oscillatoria*). The average ± SE ($n = 3$) chlorophyll content in this biofilm was 45.0 ± 12.2 µg Chl *a* g^{-1}.

Content of Organic Matter and Pigment

Organic matter and pigment contents were estimated separately for the oxic and underlying layers (Fig. 7A, B). For these two parameters, layer differences and seasonal differences were determined by 2-way ANOVAs. The amount of organic matter was significantly higher in the topmost 2 mm of the microbial mat, where photoautotrophic cyanobacteria dominated in biomass (Fig. 7A) regardless of the season (2-way ANOVA $F(1,7) = 1254.09$, $p < 0.001$). The underlying sediment presented on average 36% and 77% less organic matter that the topmost 2 mm, for Austral-summer and Austral-winter samples, respectively. Seasonal differences in organic-matter content were also statistically significant (2-way ANOVA $F(1,7) = 105.95$, $p < 0.001$); it is worth pointing out that

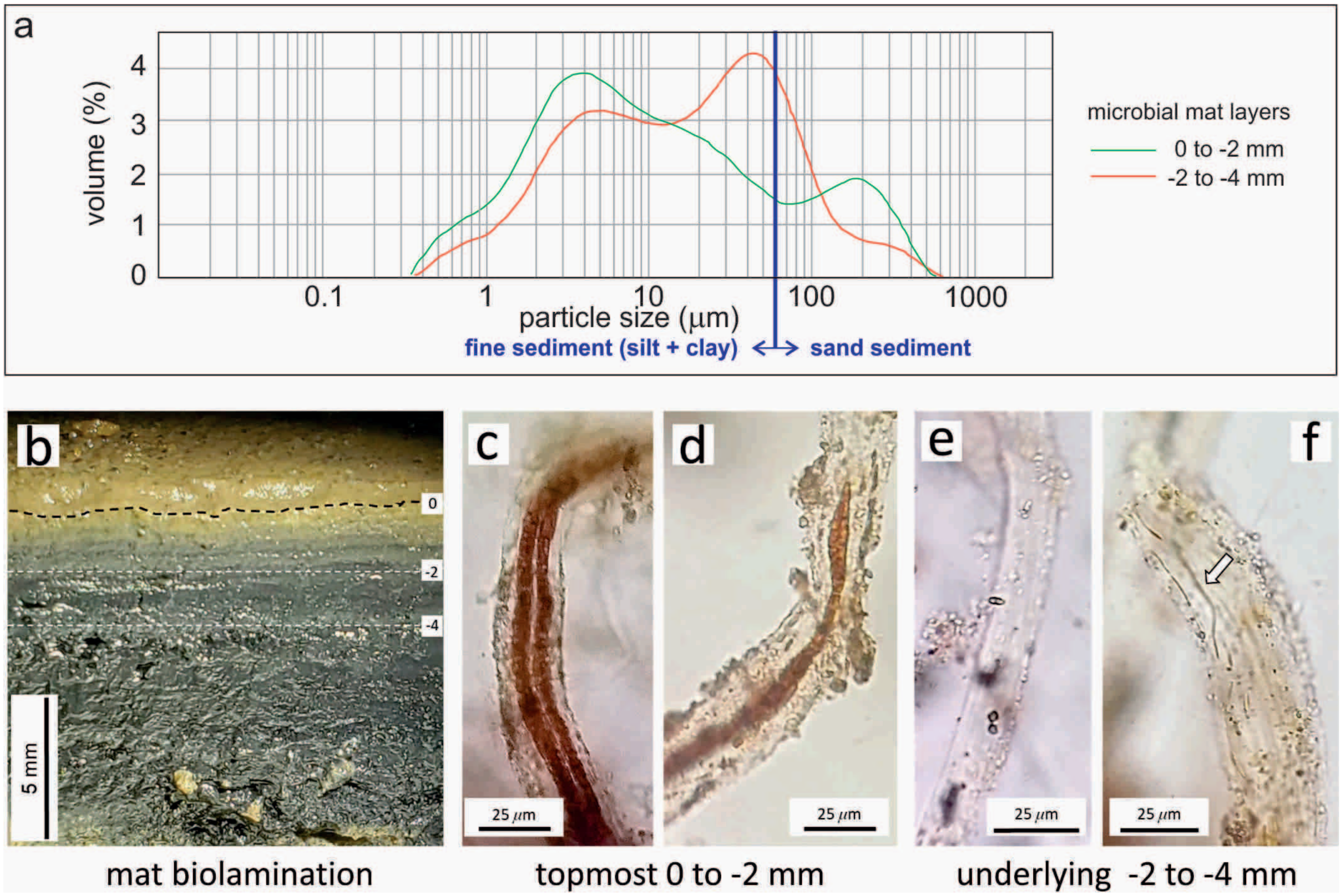

Fig. 6.—**A)** Laser-diffraction granulometry of 0 to –2 mm and –2 to –4 mm microbial-mat layers developed over gravels. B–F) Biosedimentary lamination and dominant cyanobacteria in a microbial mat growing on gravels. **B)** Stereomicroscope photograph of a cross-section depthprofile, showing the biosedimentary lamination. There is a clear distinction in coloration of the uppermost 0 to –2 mm, oxic and cyanobacteria-dominated layers, and the underlying anoxic strata, starting at –2 mm depth. Black dashed line marks the level of the substrate (0 mm), and white lines mark the –2- and –4-mm strata. **C, D)** Whole *Coleofasciculus chthonoplastes* trichomes that dominate in biomass in the uppermost 0 to –2 mm of the mat, showing the characteristic "braided" pattern of many filaments within a single, thick sheath. **E, F)** Empty *C. chthonoplastes* sheaths (arrow indicates some remaining filaments) that abound in the anoxic biosedimentary strata in the 2–4 mm horizon. *C. chthonoplastes* trichomes are so thick and long, and their filament tracks so convoluted, that some sections appear out of focus in the same picture. Brownish coloration of filaments (in Parts C and D) is due to the use of acidic Lugol's solution as a preservative. Mud sediment particles are attached to external sheath and EPS aggregations. All photomicrographs (C–F) taken at 400 × magnification.

organic-matter content was comparable in sediment layers below –2 mm, regardless of the season.

Regarding the content in chlorophyll *a*, the concentration for the uppermost 2 mm where cyanobacteria dominated in abundance was significantly higher than in underlying layers (2-way ANOVA $F(1,11) = 4003.19$, $p < 0.001$), presenting quite elevated values that on average (± SE) were 94.5 ± 5.6 and 425.7 ± 2.4 μg Chl *a* g^{-1} sediment for Austral-summer and Austral-winter samples, respectively (Fig. 7C). The proportional drop in pigment content in the underlying layers (–2 to –10 mm) corresponded to 85% and 518% for Austral summer and winter, respectively. As in the case of organic matter, pigment content was comparable in the underlying anoxic sediments (–2 to –10 mm) for Austral-summer and Austral-winter samples, indicating that the largest seasonal variation in pigment took place in the cyanobacteria-dominated uppermost layers. These marked seasonal differences in pigment content were statistically significant (2-way ANOVA $F(1,11) = 3040.56$, $p < 0.001$). Furthermore, the aspect of epibenthic microbial mats growing on gravel deposits presents contrasting characteristics in Austral summer (Fig. 7C, left) *vs.* winter (Fig. 7C, right). In the former case, the mat extending between exposed pebbles looked like an even, leathery parchment; in Austral winter, large areas of the epibenthic mat produced bubbles.

In comparison, the mat rim lacked a layered pattern, and was 3–4 mm thick (see Fig. 4D). Its average organic matter content (n = 4 ± SE) was 22.61 ± 1.1%, a value comparable to the uppermost 2 mm of its adjacent well-developed mat (see Fig. 7A for graphic comparison). The average pigment content of this rim (n = 4 ± SE) was 150.1 ± 34.4 μg Chl *a* g^{-1} sediment, which by contrast to its organic-matter content, represents a value 2.8-fold lower than that for the uppermost 2 mm of the adjacent mat in Austral winter, yet 1.6-fold larger than the mat in Austral summer (see Fig. 7B for graphic comparison).

DISCUSSION

The sedimentary mosaic at Paso Seco creates areas of positive topographic relief where gravel accumulations become largely exposed, acting in an analogous way as a supratidal environment due to the recurrent supply of seawater that takes place episodically only during storm events. Thus, the seasonal sampling of microbial mats and continuous monitoring of seawater flooding carried out in this study provides empirical support that microbial processes and sedimentary dynamics interact leading up to

TABLE 1.—*Microbiological analysis of diatom species, typified according to their habitat preference, lifeform, and salinity tolerance, and their relative abundance in samples. Reference to abbreviations SUM, Austral-summer samples; WIN, Austral-winter samples; 0 to –2 mm and –2 to –4 mm refer to the uppermost 2 mm, and the underlying 2 mm of the microbial mat, respectively; rim, 3-mm-thick "advance" border of pebble-encroaching mat; scraping, samples obtained by scraping the uncovered surface of individual pebbles.*

Diatom Group	Species	Habitat	Lifeform	Salinity	SUM 0/–2 mm	WIN 0/–2 mm	WIN –2/–4 mm	SUM Rim	WIN Rim	WIN Scraping
pennate/raphid	*Achnanthes brevipes*	aquatic	epiphytic	marine–brackish						
"	*Amphora* sp.		epiphytic, epipelic	marine						
"	*Amphora copulata*	periodic water or wet subaereal	benthic, epiphytic	brackish/freshwater			**			
"	*Caloneis* sp.		epipelic	marine–brackish						
"	*Cylindrotheca closterium*	aquatic	tychoplankton	marine						
"	*Diploneis* sp.		epipelic	marine–brackish			**			**
"	*Diploneis interrupta*	periodic water or wet subaereal	benthic, aerophilous	marine–brackish						
"	*Gyrosigma spenceri*	aquatic	epipelic	marine–brackish			**		***	**
"	*Navicula arenaria*	aquatic	benthic	marine–brackish				**		
"	*Navicula cuspidata*	periodic water or wet subaereal	benthic	brackish					**	
"	*Navicula gregaria*	periodic water or wet subaereal	benthic	brackish	***					
"	*Navicula phyllepta*	aquatic	epipelic	marine–brackish	***				**	
"	*Nitzschia palea*	moist subaereal	benthic, epipelic	brackish/freshwater			**	***	***	***
"	*Nitzschia sigma*	periodic water or wet subaereal	epipelic	marine–brackish		***	***	***	***	***
"	*Pinnularia* sp.		aerophilus	brackish					**	*
pennate/araphid	*Rhaphoneis amphiceros*	aquatic	tychoplankton	marine						**
"	*Rhopalodia gibberula*		epiphytic	marine–brackish					**	
"	*Rhopalodia musculus*		epiphytic	brackish			**			
centric	*Cyclotella striata*	periodic water or wet subaereal	tychoplankton	brackish					*	
"	*Paralia sulcata*	aquatic	tychoplankton	marine/marine–brackish					**	

*** dominant
** abundant
* rare

the formation of the mats. The processes involved are: 1) frequent flooding by seawater depositing sand-size material onto the pebbles, 2) fallout of mud-size sediment particles suspended in stagnant water, 3) anchoring of a biofilm fabric in sand and baffling and trapping of fine sediment by a rapidly growing microbial mat. The cyclical alternation between flooding of the microbial mat surface and latency periods of stagnation (resulting in seawater availability and moisture maintenance) and subaerial exposure determine the timing and pattern of microbial colonization of gravel. In that sense, seasonal variation in the stagnant seawater and groundwater level seem to be determinant factors for seasonal growth of epibenthic mats. During periods of stagnant-seawater coverage (Austral winter) a biofilm grows over pebbles. The growth mechanism involves the sequentially engulfing of individual pebbles that become embedded in the mat fabric. Both the elevated organic matter and pigment contents of the rim border show a metabolically active diatom biofilm, with the capacity for rapid growth and cell division that may entrap the pebble.

The bimodal size distribution of sediment incorporated into the microbial mat is a clear reflection of the two hydrodynamic conditions that alternate in the sediment flat. On the one hand, flooding by seawater transports and deposits the larger fractions (i.e., sand-size material), while mud-size sediment particles settle out of suspension when seawater becomes stagnant. The presence of epipelic and tychoplanktonic diatoms in microbiological samples corroborates the importance of flooding currents in the resuspension and transport of microbes over the sediment flat (Delgado et al. 1991; Vos and de Wolf 1993; Huault et al. 1994; Lucas et al. 2001; Koh et al. 2006). Furthermore, by analogy with microbial communities found in other environments (Fayó et al. 2020), the occurrence of aerophilous species and others characteristic of periodic water or moist–wet subaerial habitats, points to the alternating pulses of flooding, water stagnation, and desiccation to which this environment is subject, and the role that water availability plays in shaping up microbial communities.

The processes of microbial baffling, trapping, and binding of fine sediment grains lead to sediment accretion in microbial mats (Noffke et al. 2001; Walter and Allwood 2005). Our findings suggest that trapping and baffling of sediments jointly with increment in biomass takes place during periods of water stagnation (~ 14 days and longer). The water stagnation is longer during Austral-winter months (see inset in Fig. 3A), when groundwater level remains closer to the sediment flat. Therefore, it is reasonable to assume that water availability promotes biomass enrichment, indicated by the statistically significant differences in chlorophyll *a* and organic matter content in the uppermost 2 mm of the mat (Fig. 7A, B). Baffling and trapping of microbial sediment levels the depositional surface. The accumulation of empty cyanobacteria sheaths in older (deeper) and anoxic layers of the mat (Fig. 6E, F) together with active secretion of EPS (extracellular polymeric substances) by raphid diatoms contributes to increasing cohesion of the mat (Gerdes 2007). Furthermore, a large proportion of the organic matter in microbial mats is derived from the accumulation of colloidal exopolymers and empty cyanobacterial sheaths in anoxic layers, the latter being recalcitrant to chemical and microbial degradation (Fenchel and Kühl 2000; de los Ríos et al. 2004; Stal 2010). In that sense, the biostabilization causes MISS such as fold-overs, rips, and tears (Fig. 2A, B, D). Likewise, negative molds (Fig. 2D) originally

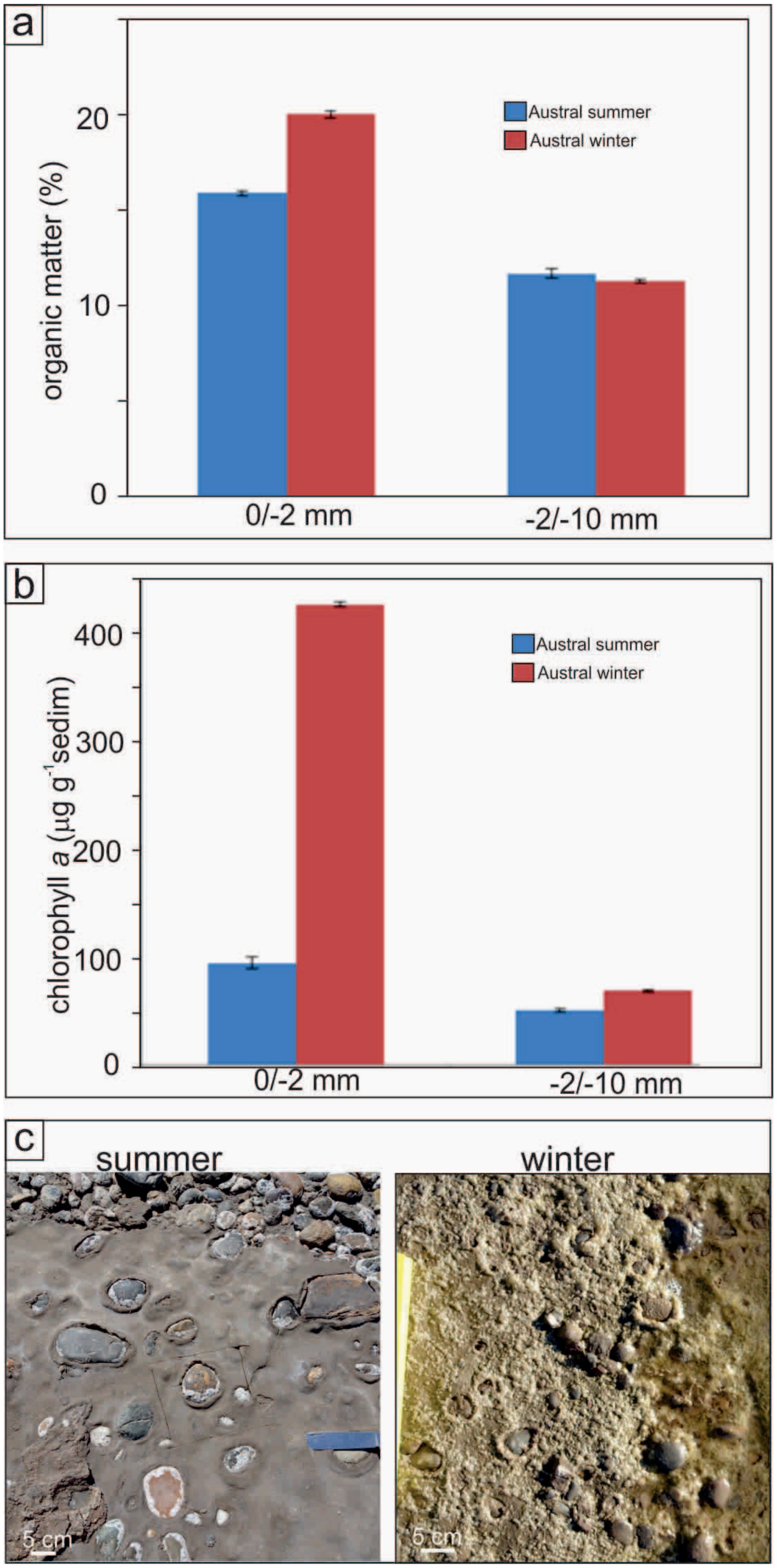

Fig. 7.—Seasonal variation in the distribution of organic matter and photosynthetic pigment. **A)** Organic-matter content in the oxic (0 to –2 mm) and underlying anoxic horizons (–2 to –10 mm) of microbial mats colonizing gravel deposits; from Austral-summer (December) and Austral-winter (July) samples. Bars represent average values ± SE. **B)** Idem for chlorophyll *a*. **C)** Photographs show epibenthic microbial mat growing on gravel deposits, from which samples were taken for analyses. General appearance of the study site in Austral summer (December) *vs*. Austral winter (July).

imprinted by pebbles in the overlying mat document biostabilization properties.

The stagnant water column of a few centimeters depth (or even a thin lamina of overlying seawater) provides an adequate environment for microbial growth. Microbes rely on surface adherence for the creation of biofilms and the early colonization of substrates (Hall-Stoodley et al. 2004; 1 in Fig. 5D). In fact, genes involved in the regulation or expression of surface-adhesion proteins and EPS characterize the early stages of biofilm formation (Hall-Stoodley et al. 2004). Furthermore, the EPS matrix displays important viscoelastic properties in response to an applied force as a water current (Peterson et al. 2015; Decho and Gutierrez 2017) maintaining the biofilm attached to the pebbles (see video 1 in Supplemental Material). Despite the delicate nature of pioneering biofilms, the architectural framework created by EPS can give the matrix physical stability to hydrodynamic disturbances. Pebble colonization proceeds even after the overlying stagnant water lamina has evaporated, as water molecules create a hydrosphere around sediment grains through surface-tension moistening otherwise dry surfaces (Stoodley 2016; Fig. 5E, F).

Diatoms are the dominant fraction of primary producers on exposed pebble surfaces as biofilm, found from the microbiological analysis of surface scrapings, while filaments of cyanobacteria such as *Leptolyngbya* and *Oscillatoria* may be embedded in this biofilm. It may be stated that diatom-dominated biofilms constitute the first stage of colonization, whereas epibenthic microbial mats represent mature stages. The marked differences in pigment content between diatom-dominated biofilms and epibenthic microbial mats, or the rim that develops around individual pebbles (which are an order of magnitude higher in mats *vs*. biofilms), point out the early role of these biofilms that develop first on the exposed surfaces of individual pebbles and are later encroached by mats. Thus, diatom biofilms may act as so-called "conditioning" biofilms in modern microbial-mat colonization of gravel deposits. The existence of primordial "conditioning" biofilms has recently been presented and discussed by Talluri et al. (2020), and diatom substratum adhesion mediated by extracellular proteoglycans has long been recognized (Lind et al. 1997). Likewise, Pan et al. (2017) experimentally found that pennate diatom biofilms act as opportunistic colonizers in sediments. Once individual pebbles are covered by a biofilm, inherent biological features of filamentous cyanobacteria, their motility and capacity for vertical and horizontal migration through sediment layers, and their attachment to surfaces makes them pioneering colonizers of pebbles.

CONCLUSIONS

Microbial-mat development over gravel deposits is herein related to a variety of hydro- and sediment-dynamic conditions. The sequential stages of microbial colonization of gravel start with pioneering biofilms that ultimately contribute to the formation and become an integral part of cohesive, layered epibenthic microbial mats. With increasing coherence, the developing microbial mat may encroach onto individual pebbles, ultimately engulfing them. The sedimentary surface affected by cycles of flooding, stagnation, followed by subaerial exposure and desiccation, is the key to colonize gravel substratum. The hydric regime, of which the creation of a shallow, stagnant water column appears to be of primary importance, controls microbial growth over pebbles, and consequently biomass accumulation in biofilm formation. On par, baffling and trapping accumulates fine-grained material in the developing mat matrix. Mature, layered mats may encroach pebbles until they become completely covered and the micro-topographic differences in the sedimentary flat are levelled. Once epibenthic microbial mats are established, MISS may be formed through rupture and redeposition of the cohesive mats during episodic storm surges.

SUPPLEMENTALMATERIAL

Supplemental material is available from the SEPM Data Archive: https://www.sepm.org/supplemental-materials.

ACKNOWLEDGMENTS

The authors declare no potential conflict of interest. Authors acknowledge the collaboration of L.A. Raniolo (field sampling) and J. Carbonella (granulometry analysis). Funding for this research came through grants PICT 19-4253 (awarded to JP) and PICT 19-2182 (awarded to DGC) from ANPCyT; and PGI 24/H081 (awarded to DGC) from the SECyT UNS.

REFERENCES

Blakemore, L.C., Searle, P.L., and Daly, B.K., 1987, Methods for chemical analysis of soils: New Zealand Soil Bureau, Scientific Report 80, 103 p.

Bolhuis, H., and Stal, L.J., 2011, Analysis of bacterial and archaeal diversity in coastal microbial mats using massive parallel 16S rRNA gene tag sequencing: International Society for Microbial Ecology, Journal, v. 5, p. 1701–1712.

Cuadrado, D.G., and Pan, J., 2018, Field observations on the evolution of reticulate patterns in microbial mats in a modern siliciclastic coastal environment: Journal of Sedimentary Research, v. 88, p. 24–37.

Cuadrado, D.G., Pan, J., Gómez, E.A., and Maisano, L., 2015, Deformed microbial mat structures in a semiarid temperate coastal setting: Sedimentary Geology, v. 325, p. 106–118.

Decho, A.W., and Gutierrez, T., 2017, Microbial extracellular polymeric substances (EPSs) in ocean systems: Frontiers in Microbiology, v. 8, p. 922, doi: 10.3389/fmicb.2017.00922.

de los Ríos, A., Ascaso, C., Wierzchos, J., Fernández-Valiente, E., and Quesada, A., 2004, Microstructural characterization of cyanobacterial mats from the McMurdo Ice Shelf, Antarctica: Applied and Environmental Microbiology, v. 70, p. 569–580.

Delgado, M., de Jonge, V.N., and Peletier H., 1991, Experiments on resuspension of natural microphytobenthos populations: Marine Biology, v. 108, p. 321–328.

Denys, L., 1991, A check-list of the diatoms in the Holocene deposits of the western Belgian coastal plain with a survey of their apparent ecological requirements, Volume I: Introduction, ecological code and complete list: Service Geologique de Belgique, no. 246, 41 p.

Edgcomb, V.P., Bernhard, J.M., Summons, R.E., Orsi, W., Beaudoin, D., and Visscher, P.T., 2014, Active eukaryotes in microbialites from Highborne Cay, Bahamas, and Hamelin Pool (Shark Bay), Australia: The International Society for Microbial Ecology, Journal, v. 8, p. 418–429.

Espinosa, M.A., and Isla, F.I., 2011, Diatom and sedimentary record during the mid-Holocene evolution of the San Blas estuarine complex, northern Patagonia, Argentina: Ameghiniana, v. 48, p. 411–423.

Fayó, R., Pan, J., and Espinosa, M.A., 2020, Microbial mat and surface sediment communities from a shallow oxbow lake in the Colorado River floodplain, Argentina: Geomicrobiology Journal, v. 37, p. 937–949.

Fenchel, T., and Kühl, M., 2000, Artificial cyanobacterial mats: growth, structure, and vertical zonation patterns: Microbial Ecology, v. 40, p. 85–93.

Ferrelli, F., Bohn, V.Y., and Piccolo, M.C., 2012, Variabilidad de la precipitación y ocurrencia de eventos secos en el sur de la provincia de Buenos Aires (Argentina): IX Jornadas Nacionales de Geografía Física, Proceedings, p. 15–28.

Frantz, C.M., Petryshyn, V.A., and Corsetti, F.A., 2015, Grain trapping by filamentous cyanobacterial and algal mats: implications for stromatolite microfabrics through time: Geobiology, v. 13, p. 409–423.

Gerdes, G., 2007, Structures left by modern microbial mats in their host sediments, *in* Schieber, J., Bose, P.K., Eriksson, P.G., Banerjee, S., Sarkar, S., Altermann, W., and Catuneau, O., eds., Atlas of Microbial Mat Features Preserved within the Clastic Rock Record: Elsevier, p. 5–38.

Hall-Stoodley, L., Costerton, J.W., and Stoodley, P., 2004, Bacterial biofilms: from the natural environment to infectious diseases: Nature Reviews Microbiology, v. 2, p. 95–108.

Huault, M.F., Lafite, R., and Dupontt, J.P., 1994, Diatoms as particulate tracers in the water column in the eastern English channel: Netherlands Journal of Sea Research, v. 33, p. 47–56.

Kaźmierczak, J., Fenchel, T., Kühl, M., Kempe, S., Kremer, B., Łacka, B., and Małkowski, K., 2015, $CaCO_3$ precipitation in multilayered cyanobacterial mats: clues to explain the alternation of micrite and sparite layers in calcareous stromatolites: Life, v. 5, p. 744–769.

Koh, C.-H., Khim, J.S., Araki, H., Yamanishi, H., Mogi, H., and Koga, K., 2006, Tidal resuspension of microphytobenthic chlorophyll *a* in a Nanaura mudflat, Saga, Ariake Sea, Japan: flood–ebb and spring–neap variations: Marine Ecology Progress Series, v. 312, p. 85–100.

Komárek, J., and Hauer, T., 2013. CyanoDB.cz, On-Line Database of Cyanobacterial Genera: Word-Wide Electronic Publication: University of South Bohemia and Institute of Botany, http://www.cyanodb.cz.

Lind, J.L., Heimann, K., Miller, E.A., van Vliet, C., Hoogenraad, N.J., and Wetherbee, R., 1997, Substratum adhesion and gliding in a diatom are mediated by extracellular proteoglycans: Planta, v. 203, p. 213–221.

Lorenzen, C.J., 1967, Determination of chlorophyll and pheopigments: spectrophotometric equations: Limnology and Oceanography, v. 12, p. 343–346.

Lucas, C.H., Banham, C., and Holligan, P.M., 2001, Benthic–pelagic exchange of microalgae at a tidal flat. 2. Taxonomic analysis: Marine Ecology Progress Series, v. 212, p. 39–52.

Maisano, L., Spagnuolo, J.O., and Cuadrado, D.G., 2016, Caracterización sedimentológica de una planicie costera colonizada por microorganismos: XV Reunión Argentina de Sedimentología, Proceedings, p. 112.

Maisano, L., Cuadrado, D.G., and Gómez, E.A., 2019, Processes of MISS-formation in a modern siliciclastic tidal flat, Patagonia (Argentina): Sedimentary Geology, v. 381, p. 1–12.

Martínez, O.A., and Kutschker, A., 2011, The "Rodados Patagónicos" (Patagonian shingle formation) of eastern Patagonia: environmental conditions of gravel sedimentation: Biological Journal of the Linnean Society, v. 103, p. 336–345.

Martinez, O., Rabassa, J., and Coronato, A., 2009, Charles Darwin and the first scientific observations on the Patagonian shingle formation (Rodados Patagónicos): Revista Asociación Geológica Argentina, v. 64, p. 90–100.

Noffke, N., 2000, Extensive microbial mats and their influences on the erosional and depositional dynamics of a siliciclastic cold water environment (Lower Arenigian, Montagne Noire, France): Sedimentary Geology, v. 136, p. 207–215.

Noffke, N., 2010, Geobiology: Microbial Mats in Sandy Deposits from the Archean Era to Today: Springer-Verlag, 205 p.

Noffke, N., Gerdes, G., Klenke, T., and Krumbein, W.E., 1997, A microscopic sedimentary succession indicating the presence of microbial mats in siliciclastic tidal flats: Sedimentary Geology, v. 110, p. 1–6.

Noffke, N., Gerdes, G., Klenke, T., and Krumbein, W.E., 2001, Microbially induced sedimentary structures: a new category within the classification of primary sedimentary structures: Journal of Sedimentary Research, v. 71, p. 649–656.

Pan, J., 2021, Microbes and marine sediments: a life-long relationship on Earth's Biosphere, *in* Hurst, C.J., ed., Microbes: The Foundation Stone of the Biosphere: Springer, Nature 8, p. 57–88.

Pan, J., Cuadrado, D.G., and Bournod, C.N., 2017, Diatom-driven recolonization of microbial mat-dominated siliciclastic tidal flat sediments: Federation of European Microbiological Societies, Microbiology Ecology, v. 93, fix111.

Perillo, V.L., Maisano, L., Martinez, A.M., Quijada, I.E., and Cuadrado, D.G., 2019, Microbial mat contribution to the formation of an evaporitic environment in a temperate-latitude ecosystem: Journal of Hydrology, v. 575, p. 105–114.

Peterson, B.W., He, Y., Ren, Y., Zerdoum, A., Libera, M.R., Sharma, P.K., van Winkelhoff, A., Neut, D., Stoodley, P., van der Mei, H.C., and Busscher, H.J., 2015, Viscoelasticity of biofilms and their recalcitrance to mechanical and chemical challenges: Federation of European Microbiological Societies, Microbiology Reviews, v. 39, p. 234–245.

Rutter, N., Schnack, E.J., del Rio, J., Fasano, J.L., Isla, F.I., and Radtke, U., 1989, Correlation and dating of Quaternary littoral zones along the Patagonian coast, Argentina: Quaternary Science Reviews, v. 8, p. 213–234.

Stal, L.J., 2010, Microphytobenthos as a biogeomorphological force in intertidal sediment stabilization: Ecological Engineering, v. 36, p. 236–245.

Stal, L.J., van Gemerden, H., and Krumbein, W.E., 1985, Structure and development of a benthic marine microbial mat: Federation of European Microbiological Societies, Microbiology Ecology, v. 31, p. 111–125.

Stempels Bautista, C., Cuadrado, D.G., and Piccolo, M.C., 2019, Efecto de las ondas de tormenta en un estrecho de marea (Paso Seco, Buenos Aires): XVIII Congreso Latinoamericano de Ciencias del Mar, Proceedings, p. 776.

Stoodley, P., 2016, Biofilms: flow disrupts communication: Nature Microbiology, v. 1, no. 15012, doi.org/10.1038/nmicrobiol.2015.12.

Talluri, S.N.L., Winter, R.N., and Salem, D.R., 2020, Conditioning film formation and its influence on the initial adhesion and biofilm formation by a cyanobacterium on photobioreactor materials: Biofouling, v. 36, p. 183–199.

Trebino, L.G., 1987, Geomorfología y evolución de la costa en los alrededores del pueblo de San Blas, provincia de Buenos Aires: Revista Asociación Geológica Argentina, v. 42, p. 9–22.

Vos, P.C., and de Wolf, H., 1993, Diatoms as a tool for reconstructing sedimentary environments in coastal wetlands: methodological aspects: Hydrobiologia, v. 269–270, p. 285–296.

Walter, M.R., and Allwood, A.C., 2005, Biosediments and biofilms, *in* Selly, R.C., Cocks, L.R.M., and Plimerm, I.R., eds., Encyclopedia of Geology: Elsevier, p. 279–294.

Watermann, F., Hillebrand, H., Gerdes, G., Krumbein, W.E., and Sommer, U., 1999, Competition between benthic cyanobacteria and diatoms as influenced by different grain sizes and temperatures: Marine Ecology Progress Series, v. 187, p. 77–87.

Witte, L., 1916, Estudios geológicos de la región de San Blas (Partido de Patagones) con especial atención a los depósitos de pedregullo que se hallan en la costa: Museo de La Plata, Revista, v. 24, p. 7–99.

Received 16 March 2022; accepted 29 April 2022.